World Journal of Advanced Research and Reviews
eISSN: 2581-9615 CODEN (USA): WJARAI
Cross Ref DOI: 10.30574/wjarr
Journal homepage: https://wjarr.com/

(RESEARCH ARTICLE)

Check for updates

Design parameters for fluid flow simulation through mesh wick structures for thermal compressor systems

Ifeanyi Augustine Uwaoma [1,*] and Olusegun Abiodun Balogun [2]

[1] *Department of Mechanical Engineering, School of Mechanical, Industrial and Manufacturing Engineering (MIME), Oregon State University, Corvalis, USA*
[2] *Department of Mechanical Engineering, College of Engineering and Technology (CoTEC), Jomo Kenyatta University of Agriculture and Technology, Nairobi, Kenya.*

World Journal of Advanced Research and Reviews, 2024, 23(01), 753–764

Publication history: Received on 18 May 2024; revised on 03 July 2024; accepted on 06 July 2024

Article DOI: https://doi.org/10.30574/wjarr.2024.23.1.2020

Abstract

This research explores the transportation of a working fluid within a mesh wick structure at velocity of 12m/s. The research examines the influence of key design parameters on fluid flow through the mesh wick structure. By investigating these parameters, insights can be gained into optimizing the design for efficient fluid transport. This study investigates the thermal and fluid dynamics within a cylindrical mesh wick housing composed of aluminum and copper mesh materials. The wick structure comprises an inlet and outlet part, with four porous materials assembled together. By discretizing governing equations of continuity, momentum, and energy over the flow domain using Finite Volume-based equations in Ansys, accurate simulation results were obtained. An extra fine fluid mesh was employed to simulate conjugate heat transfer phenomena effectively. Temperature distribution within the porous wick revealed varying profiles, highlighting localized temperature variations near the outlet nozzle. Pressure distribution showed a gradient influenced by swirling velocities within the vortex at the inlet. Boundary heat flux sensible analysis demonstrated its significant impact on heat distribution and thermal management processes. Velocity profiles showcased uniformity at the inlet and increased velocity at the outlet, indicating the influence of porous wick on fluid flow dynamics. Overall, this research enhances understanding of thermofluidic flow through porous wick materials, crucial for optimizing thermal management systems and energy conservation processes.

Keywords: Fluid Flow; Mesh Wick Structure; Heat Transfer; Thermal Compressor; Fluid Velocity

1. Introduction

A heat pipe is a passive heat transfer device characterized by high thermal conductance, utilizing the solid enclosure's thermal conduction and the internal working fluid's phase change (Marchal, J. M., , 2001). The working fluid circulates passively within the heat pipe, transferring heat from the evaporator to the condenser region through convective heat transfer and phase change phenomena (Attinger et al. 2014). Initially explored for space applications, they are now extensively researched for cooling high heat-density systems in the electronics industry (Garimella et al. 2016). Additionally, there is active discussion regarding their use in large-scale systems, such as enhancing solar cell efficiency (Wadia et al. 2009) and serving as passive cooling systems for nuclear power plants during beyond design-basis accidents (Mull et al., 2022). Recent research focuses on liquid metal heat pipes with annular wick structures, particularly for application in micro nuclear reactors (Seo et al. 2022). Moreover, the surrounding environment, including air, lakes, and seas, could potentially serve as heat sinks for the Earth's micro reactors.

* Corresponding author: Ifeanyi Augustine Uwaoma

Percolation refers to the outward movement of water horizontally or vertically through a flexible material (Wemp and Carey, 2017). This movement is driven by surface gravity, cohesion of the liquid, and intermolecular attraction between the liquid surface and the solid surface under wet or wet conditions (Barnes and Umugwaneza, 2011). Moisture plays an important role in cracking as it determines the ability of soft materials to handle water (Li et al., 2023). Although volatility and volatility are different things, they both affect water vapor responding to capillary pressure. Wettability refers to the behavior of the network with the active liquid, while wettability refers to the continuous flow in the capillary pores (Harnett and Mehta, 1984). It has various applications in different fields such as wake-up, oil processing, printing, pharmaceutical use and thermal management systems. Low conductivity is important in heat exchangers used in electronics and nuclear energy (Hasan, 2020).

The ability to move water through the pore system affects the roughness of the soil surface, gravity, shear strength, and evaporation rate in the meniscus (Masoodi and Pillai, 2013). Advances in nanotechnology have led to the production of nanostructures or microstructures, allowing researchers to better understand capillary growth in various structures such as nanoporous layers, Nano arches, nanowires, and micro/nanopillars (Wemp, 2017; Song et al., 2005; Yun et al., 2017). However, capillary rise across heat compressor nanostructures has not yet been well characterized. This study aims to simulate thermal compressor flow in knitted or mesh wick structure. It uses computational fluid dynamics (CFD) to model and simulate the flow of thermal compressor fluid through a solid network. Uwaoma, (2021) investigated various mesh sizes of both plain copper and nanostructured wicks using capillary rise experiments to determine their effectiveness in transporting mass through a thermal compressor system. The results showed that the 250-mesh nanostructured wick outperformed others, demonstrating superior capillary rise performance and pumping rates across different evaporation regimes. Statistical analysis supported this choice, attributing it to the unique surface properties of the nanostructured mesh. This selection was recommended for achieving the desired mass flow rate of 50 g/s in the thermal compressor system. The research suggests that nanostructured wicks offer prospective advantages in fluid flow optimization for thermal management applications.

2. Literature Review

Recently, two-phase materials have been developed aiming to solve thermal control problems in thin materials with high temperatures and low surface area. Among these, heat pipes (LHPs) appear to be the most effective heat transfer solution. LHPs work by exploiting liquid phase change to facilitate heat transfer and by using capillary forces to transport water (Launay et al., 2007). LHPs were introduced in the former Soviet Union in 1972, and have proven to be promising tools for load management (Maydanik, Y., 2005). Compared to similar devices such as capillary pumps (CPLs) and heat pipes, LHPs offer many advantages, such as greater heat transfer ability, larger capacity on a comparable scale, reliable operation in magnetic fields, proportional and efficient, low temperature resistance, conductivity, etc. flexible lines, less sensitivity to electrical currents, and greatly increased thermal carrying capacity over long distances (Maydanik et al., 2014). The structure of the LHP system consists of various components, including fuse, capacitor, gas and water pipes and balancing chamber. Figure 1 shows the components of the LHP system showing its main components and details.

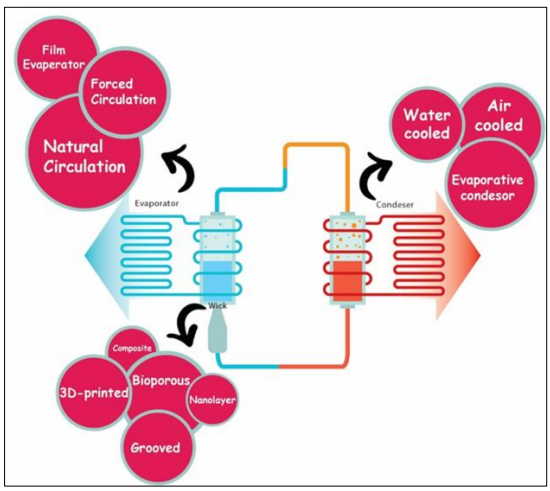

Figure 1 Categorization of different components of an LHP system based on wick structures, evaporators, and condenser.

Since the inception of Loop Heat Pipes (LHPs), their performance has been extensively examined both numerically and experimentally across numerous studies (Shi et al., 2021). Recently, researchers have conducted a review on the latest advancements in LHPs featuring flat evaporators, discussing several challenges faced by these systems. These challenges include issues such as uneven stress distribution within the casing, deformation of the evaporator due to high internal pressure, heat leakage from the evaporator into the compensation chamber, subpar startup performance, reverse flow through the wick, and continuous leakages as a result of sealing problems (Szymanski et al., 2021).

Various wick structures, such as double-pore wicks, corrugated wicks, nanolayers, composite wicks, and synthetic additives, have been evaluated and applied in LHPs to facilitate the capillary forces required for auto-diffusion of into the loop (Wu et al., 2012). In addition, these buildings play an important role in preserving the heat coming from the air and water and in the compensation gap between the air and the air (Xu et al., 2017). Figure 2 schematically illustrates the various factors contributing to increased thermal resistance.

The literature is categorized and reviewed based on existing wick structures used to enhance LHP performance, including double porous, corrugated, nanolayers, composites, and synthetic additives. To gain more insight into important variables such as heat transfer capacity and heat resistance, a wick structure that can exhibit a higher heat transfer coefficient is an obvious choice. It is interesting that most filters, including sieves and screen-lined filters, involve active industrial processes despite providing high capillary pressure and permeability (Deng et al., 2017). In contrast, additional structures such as the previous method provide a simple way to describe the geometry and properties of the nucleus (Szymanski and Mikielewicz, 2022). Considering that achieving high power transfer in LHP performance is the primary goal, future research can focus on the design and construction of fuse designs.

2.1. Theory of LHPs

LHPs are characterized as intricate systems wherein the thermal and hydrodynamic interactions among various components are closely intertwined, rendering them a viable alternative and competitor in technology (Launay & Bonjour, 2007).

The functioning of an LHP system relies on a straightforward mechanism, sharing similar physical processes with traditional heat pipes (Faghri, 2014). Essentially, LHPs work by capillary pressure in the capillary tube, keeping the heat in contact with the heat source. Applying heat to the wick causes water to evaporate from the back surface, creating a meniscus in the wick. This facilitates the transfer of air from under the microgrooves on the condenser component, using the capillary pressure created by the air flow. In this part of the LHP, displaced gases meet with radiation. The liquid transfer line facilitates the return process of adjacent liquid to the balancing chamber, enabling the engine to be filled with liquid to exhaust and maintain it at the correct level (see Figure 2). Both the water and air lines are small in diameter, making them easy to access in the limited space around the electronics. Capillary force is the force that causes fluid to flow through the system driven from the generator, eliminating the force in the LHP process.

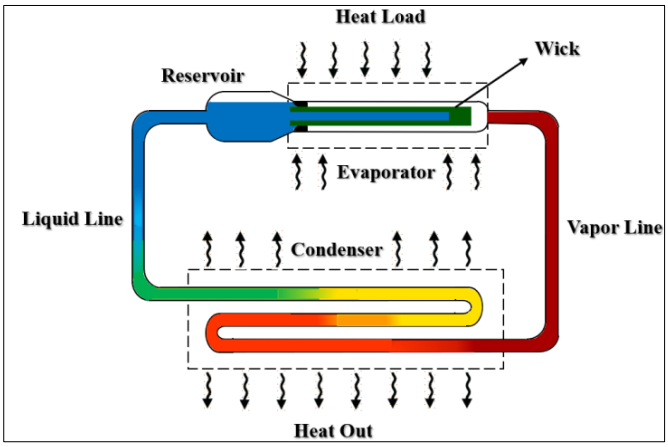

Figure 2 Main LHP geometry diagram in detail

In recent years, extensive research has focused on the performance of Loop Heat Pipes (LHPs), revealing that their efficiency is heavily influenced by factors such as the type of wicks and working fluids used. These factors are crucial in determining the operational temperature range, heat transport capacity, and overall heat transfer effectiveness of LHPs. Water has become the preferred working fluid for LHPs due to its abundant availability and high specific heat capacity, significantly impacting various efficiency aspects like startup characteristics, heat transfer coefficient, and thermal

resistance. Additionally, flat LHPs are often preferred for thermal management in both space and ground-based electronic packages due to their easy mounting on hot surfaces without requiring a saddle and their superior efficiency compared to other shapes such as disc, square, and rectangular LHPs (Chernysheva, M., Maydanik, Y., 2016). However, water may not be suitable for spacecraft applications due to the possibility of nonoperating temperatures reaching as low as -40°C. In such cases, ammonia has been proposed as a viable alternative, albeit requiring thick-walled containers to withstand the high pressures involved, which pose safety concerns for human space programs. Alternatively, acetone and ethanol, being less hazardous, are suitable for heat management of smaller electronics component dissipating heat up to approximately 100W (Li, H.; Sun, Y., 2018).

A higher acetone content offers greater advantages as an LHP liquid, especially under conditions where the reduction temperature is lowered. These benefits include reduced risk of sedimentation, operation at ambient air pressures, cheaper drilling/cleaning methods and backfill materials, and higher water temperatures. Additionally, filling the LHP with acetone results in a pressure close to atmospheric pressure, thereby minimizing the risk of leakage (Li et al., 2019). To further decrease the risk of cavitation and enhance the LHP's efficiency, ammonia is used as the working fluid (Kim and Kim, 2020). However, due to the health risks associated with ammonia, alternative working fluids are considered to mitigate these risks and broaden LHP applications. Potential alternatives include acetone, methane, methanol, and solvents containing R245fa. Currently, new working fluids such as R245fa are being tested in LHPs (Xu et al., 2021).

2.2. Wick Structures

Considering the components of the LHP system, the initial energy that powers the entire system is the capillary energy provided by the fuse. For this reason, the fuse is known as one of the most important components of the LHP system and its shape is said to be the most important factor determining the LHP performance. Therefore, structural elements are emphasized as important components in the composition of LHP, which is characterized by materials exhibiting a capillary pore structure. Permissibility, efficient use of heat, and large capillary forces occurring as functions dependent on factors such as macroscopic properties or pore size, shape, and porosity (Francisco and Lago, 2018). Key requirements for a good wick include an easy way to reduce water pressure, a low temperature to reduce the jet temperature, and sufficient capillary strength to prevent vapors from entering the water column (Tang et al., 2020). Of the categories, the dominant categories of LHP include double porous, braided, composite, composite, and synthetic additives, as shown in Figure 3 to provide a clear picture of structural categories. stainless steel, perforated steel, additive manufacturing, mesh channel processing and double mesh.

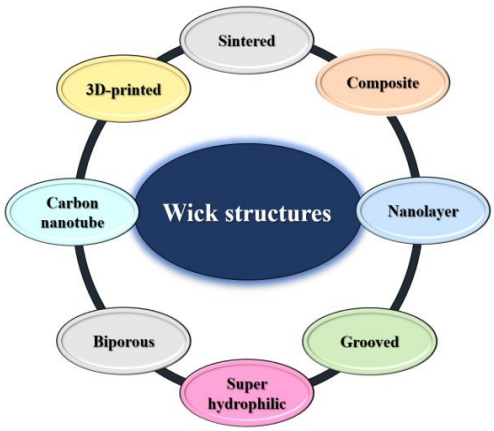

Figure 3 The most common wick types are sintered powder, metal meshes, composite wicks

3. Methodology

3.1. Model Design Assumptions

- The hot thermal compressor fluid has a constant temperature of 300K where the value of $\Delta T = 0$.
- A uniform heat flux is applied to all the walls of the tube bundle i.e $Q \neq 0$.
- The geometry of the computational domain is three-dimensional (3D) and axisymmetric.
- The fluid flow and heat transfer processes are in steady state.

The inlet velocity, V is the entrance velocity of the wick housing.

The mass flow rate ($\dot{m}$) for the flow region can be define as:

$$\rho_f V A_I = \rho_f v(N_T S_T L). \quad \text{Equation 1}$$

$$\dot{m} = \rho_f V_{max}(2A_D). \quad \text{Equation 2}$$

Using the maximum velocity, the Reynolds number can be computed as:

$$Re = \frac{\rho_f V_{max} D}{\mu_f} = \frac{V_{max} D}{v_f}. \quad \text{Equation 3}$$

$$Nu = \frac{1}{L}\int \left(-\frac{k_f}{k_f}\frac{\partial T}{\partial y}\right) dx. \quad \text{Equation 4}$$

Consideration of Fluid Properties: This section includes the equations for estimating the effective parameters that characterize the mesh wick and the base fluid. The thermal compressor effective density is defined as:

$$\rho_f = \rho_f + \rho_{sp}. \quad \text{Equation 5}$$

The thermal diffusivity:

$$\propto_f = \frac{k_f}{(\rho c_{sp})_f}. \quad \text{Equation 6}$$

where $(\rho c_{sp})_f$ is the heat capacitance.

Equation 8 can be used to calculate the effective thermal capacitance.

$$(\rho c_{sp})_f = (\rho c_{sp})_f + (\rho c_{sp})_{sp} \quad . \quad \text{Equation 7}$$

The thermal expansion coefficient of the thermal compressor fluid can also be calculated using

$$(p\beta)_f = (p\beta)_f + (p\beta)_{sp}. \quad \text{Equation 8}$$

where μ_f is the effective dynamic viscosity which can be calculated below:

$$\mu_{nf} = \frac{\mu_f}{(1-\emptyset)^{2.5}}. \quad \text{Equation 9}$$

$$k_f = k_f\left[\frac{(k_{sp}+2k_f)+2\emptyset(k_f+2k_{sp})}{(k_{sp}+2k_f)-\emptyset(k_f+2k_{sp})}\right]. \quad \text{Equation 10}$$

where k_{sp} and k_f are the thermal conductivity of mesh wick and compressor fluid respectively.

Step i: Governing Flow Equations

The governing equations for continuity, X-momentum, Y-momentum, and Energy can be expressed as:

Continuity: $\frac{\partial u}{\partial x} + \frac{\partial v}{\partial y} = 0$ Equation 11

X-Momentum: $\frac{\partial u}{\partial t} + u\frac{\partial u}{\partial x} + v\frac{\partial u}{\partial y} = \frac{1}{\rho_{nf}}\left(-\frac{\partial p}{\partial x} + \mu_f\left[\frac{\partial^2 u}{\partial x^2} + \frac{\partial^2 u}{\partial y^2}\right]\right)$ Equation 12

Y-Momentum: $\frac{\partial v}{\partial t} + u\frac{\partial v}{\partial x} + v\frac{\partial v}{\partial y} = \frac{1}{\rho_f}\left(-\frac{\partial p}{\partial y} + \mu_f\left[\frac{\partial^2 v}{\partial x^2} + \frac{\partial^2 v}{\partial y^2}\right]\right)$ Equation 13

Energy: $u\frac{\partial(\rho_f T)}{\partial x} = \frac{\mu_f}{pr_f}\frac{\partial}{\partial x}\left[\frac{\partial T}{\partial x}\right]$ Equation 14

3.2. Wick Structure Design and specification

The wick structure composes of an inlet and outlet part, four porous materials assembled together as one. Figure 4 illustrates the different components of the cylindrical mesh housing. In the longitudinal direction, the heat pipe comprises an evaporator section and a condenser section. If external geometric requirements necessitate it, an additional adiabatic section can be included to separate the evaporator and condenser. The cross-section of the heated pipe shown in Figure 4 includes the container wall, wick structure, and vapor space. Cylindrical mesh wick housing materials - Aluminum

- mesh wick housing height – 10mm
- Inlet diameter – 3mm
- Outlet diameter – 3mm
- Mesh wick materials – copper mesh

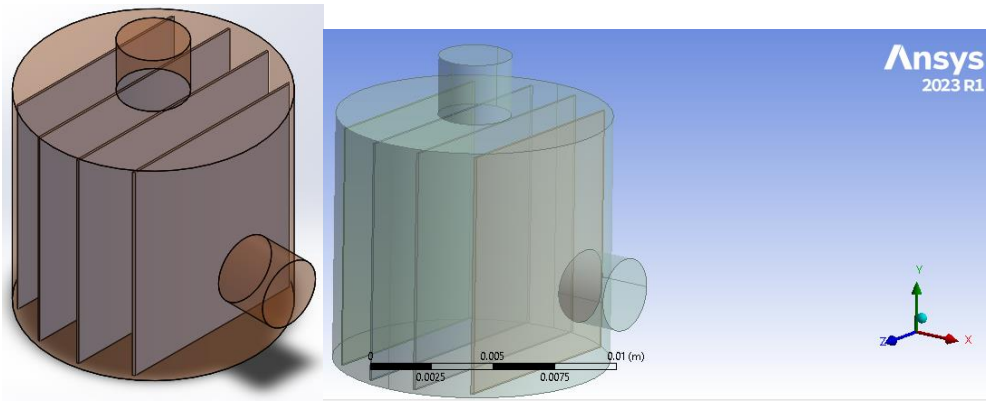

Figure 4 Mesh Wick structure design

3.3. Grid Sensitivity Analysis

To achieve well-posed simulation results, the governing equations of continuity, momentum, and energy were discretized over the flow domain of the wick structure housing. This was done using the Finite Volume method in ANSYS. A three-dimensional model was created in ANSYS, where the domain was extracted and discretized with triangular mesh elements, consisting of 98,028 elements with an edge sizing of 0.0029. The wick mesh was further divided into solid and fluid domains as illustrated in figure 5. An extra fine fluid mesh was used to simulate the conjugate heat transfer phenomenon, ensuring optimal accuracy. An extra fine mesh type was chosen in ANSYS because smaller elements reduce the distance between displaced nodes, resulting in more accurate simulation results. This approach was employed for the numerical simulation analysis in this study, thereby enhancing the results. Additionally, an analytical thermal model was developed to evaluate the generated thermofluidic flow.

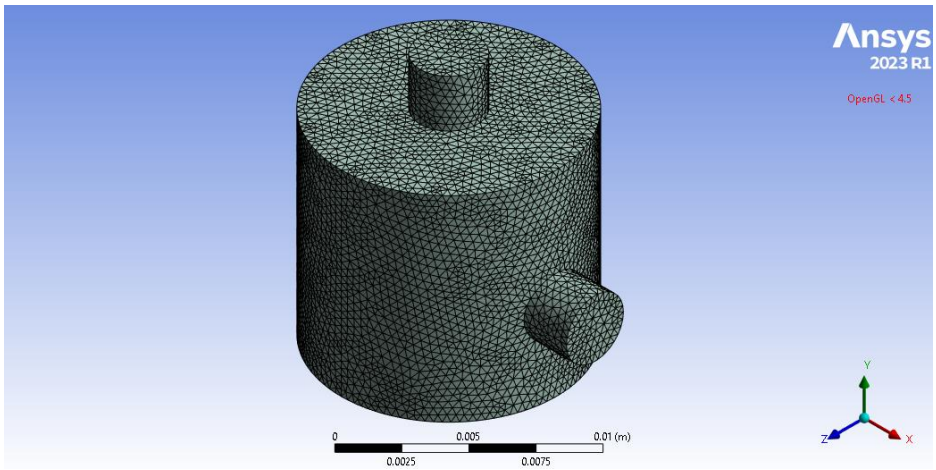

Figure 5 Mesh analysis of thermal compressor Mesh wick structure

3.4. CFD Modelling

The portrayal of temperature distribution within the porous wick employed in a thermal compressor reveals intriguing insights. Visualized through a gradient, the mesh wick exhibits varying temperature profiles, where cooler zones are depicted in blue and hotter regions in red. At the inlet, the temperature remains consistently at 300K, while the outlet maintains the same constant temperature. However, closer examination near the outlet nozzle's wall reveals a slight elevation to 302K, as illustrated in figure 6a. This observation suggests that while the wick housing sustains a uniform temperature of 300K, indicating an isothermal material characteristic, localized temperature variations occur near the outlet nozzle, potentially impacting the overall thermal performance of the system.

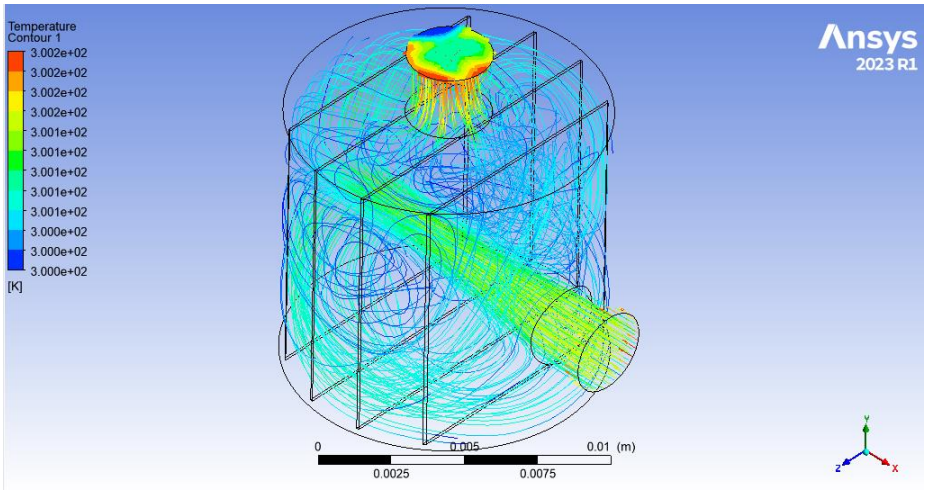

(a)

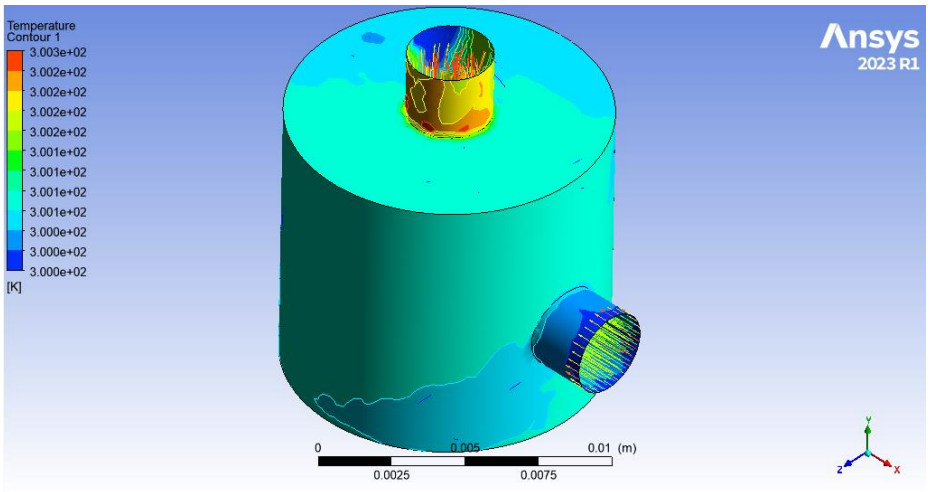

(b)

Figure 6 Temperature at the outlet

The rate of temperature change relative to displacement is equivalent to the temperature for a given direction. The average outlet temperature is 322.7 km/m and the inlet is 69.6 km/m. The temperature gradient shows a maximum in the region leaving the wick compared to the region entering the wick, as illustrated in Figure 6a and Figure 6b. The wick housing shows a heat distribution value of 15.7k/m in the area around and 322.7k/m on the wall of the unit outlet area as shown in Figure 6c.

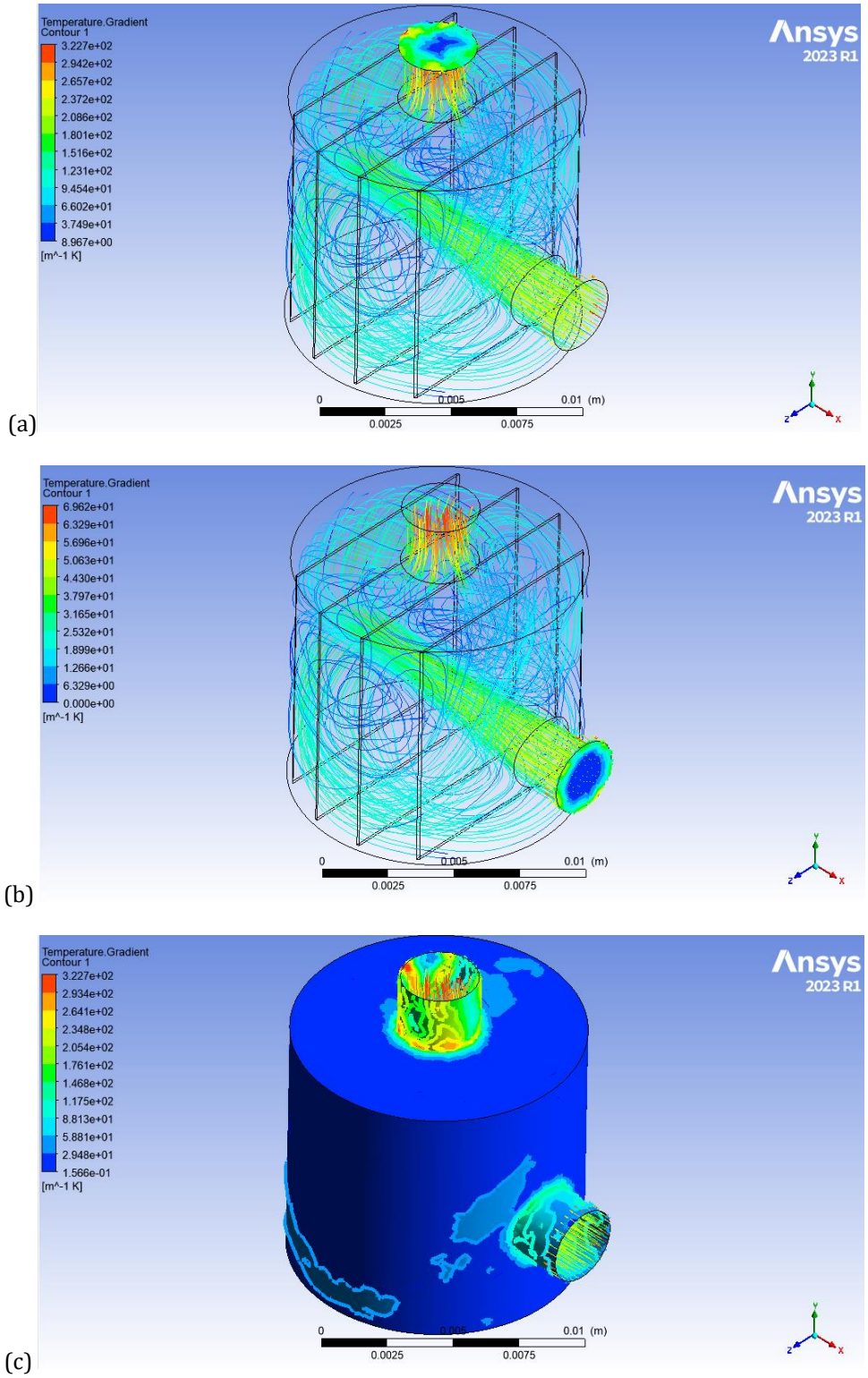

Figure 7 Temperature gradient for thermal compressor mesh wick structure

The pressure distribution reveals a gradient from the periphery towards the center, influenced by the heightened pressure zones generated by swirling velocities within the vortex at the inlet region of the wick mesh, as depicted in figure 8a. At the outlet, a consistent pressure of 61.77 Pa is observed. When pressure increases, thermofluidic flow through porous wick materials experiences alterations in velocity and distribution, potentially impacting factors such as heat transfer efficiency and fluid dynamics within the system.

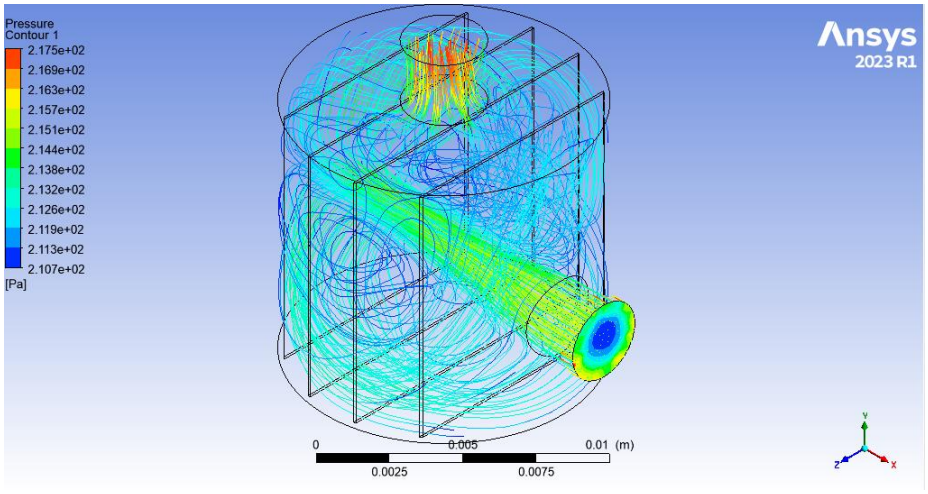

(a)

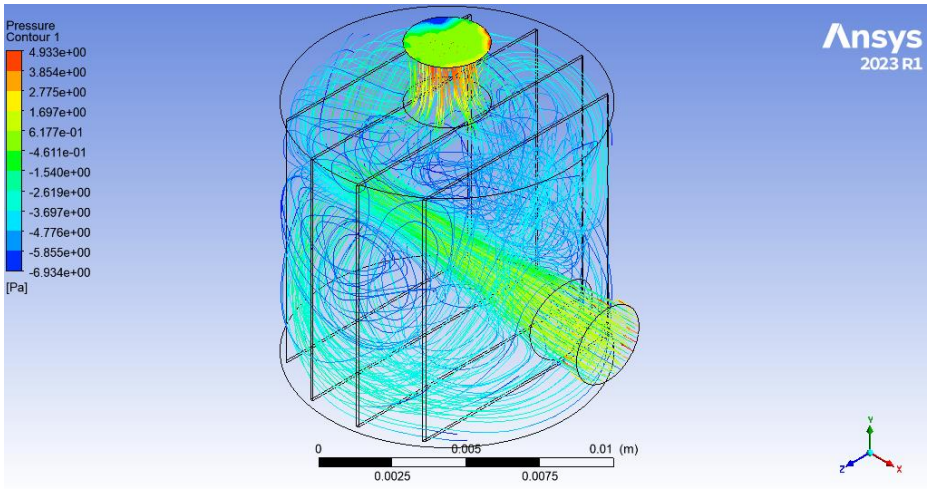

(b)

Figure 8 Pressure contour inlet, outlet and the housing for thermal compressor mesh wick structure

Boundary heat transfer is the rate of heat transfer to each unit above the boundary due to heat transfer across the boundary. Boundary heat flux sensible shows a maximum value of 7091Wm^2 having a significant effect on the heat distribution. Positive temperature yield to an increase temperature of the wick, while negative temperature causes the wick to cool for the cooling of the fluid passing through the mesh wick. This heat plays an important role in various building processes, including thermal management systems, heat exchange and conservation of energy.

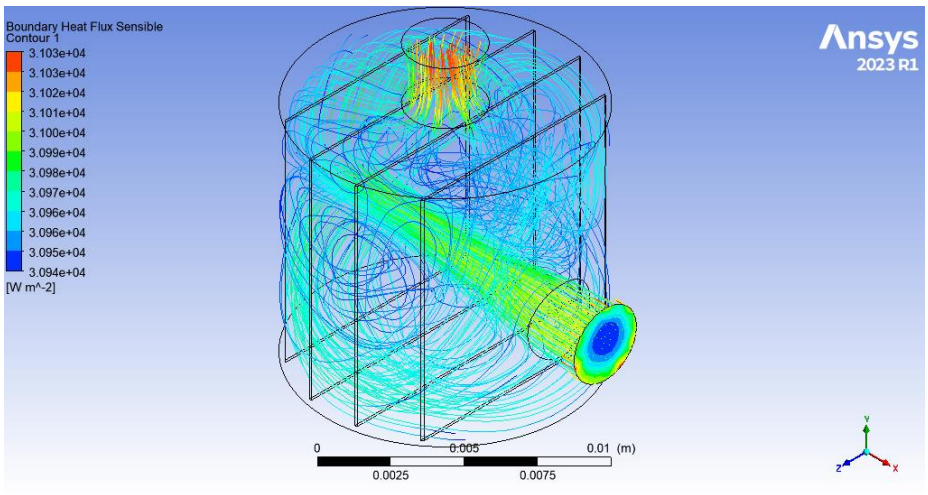

(a)

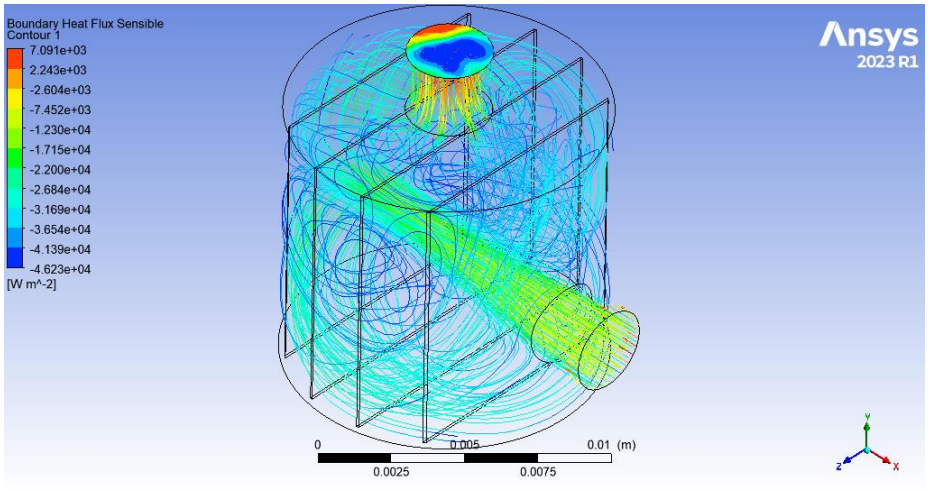

(b)

Figure 9 Boundary heat flux inlet and outlet for thermal compressor mesh wick structure

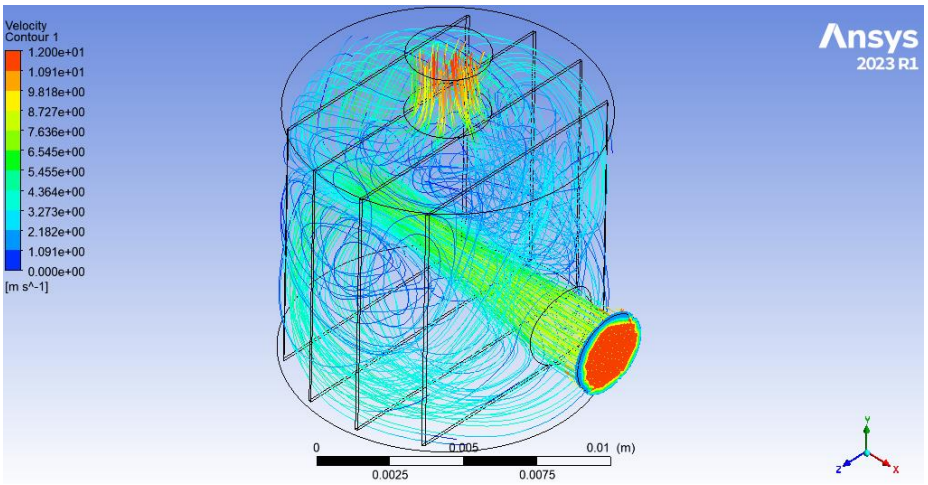

(a)

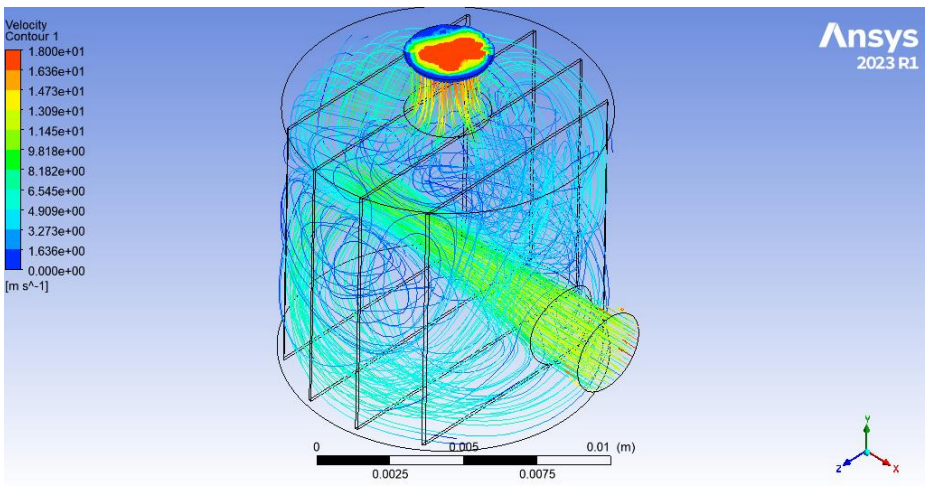

(b)

Figure 10 Velocity at the inlet and outlet

The velocity profile of the inlet shows a uniform velocity of 12m/s while the velocity value at the wall is 0m/s which shows no slip condition. The velocity at wall of a component is zero. The velocity at the outlet of the mesh wick component increased to 18m/s from 12m/s. The velocity moving to the walls of the outlet region reduces gradually towards the wall of the outlet. It was observed the velocity at the end region was enhanced, showing the presence of porous wick facilitating the velocity profile of hydrodynamic fluid flow. The velocity of thermal fluid flow is a

fundamental parameter that influences many aspects of fluid flow, including flow rate, pressure distribution, boundary layer characteristics, turbulence, and drag forces.

4. Conclusion

A design concept of a mesh wick structure used for thermal compressor system was model using Solidworks. Furthermore, numerical simulation using Fluent in ANSYS 2023 R1 was also presented on velocity profile, pressure drop contour; Boundary heat flux, Temperature and temperature gradient of thermal fluid for compressor system under steady-state laminar flow.

In this study, a cylindrical mesh wick housing composed of aluminum was investigated, featuring an inlet and outlet part with four porous materials assembled together. The primary regions of the cylindrical mesh housing, including the evaporator and condenser sections, were delineated to elucidate the heat pipe's structure. To ensure accurate simulation results, governing equations of continuity, momentum, and energy were discretized over the wick structure housing domain using Finite Volume-based equations in Ansys. The mesh wick was further discretized into solid and fluid domains, with an emphasis on extra fine fluid mesh to simulate conjugate heat transfer phenomena accurately. Analyzing temperature distribution within the porous wick revealed intriguing insights, highlighting localized temperature variations near the outlet nozzle and the uniform temperature maintenance of the wick housing. The temperature gradient was examined, showcasing maximum values at the outlet region compared to the inlet. Pressure distribution exhibited a gradient from the periphery towards the center, with heightened pressure zones influenced by swirling velocities within the vortex at the inlet. Boundary heat flux sensible was analyzed, indicating its significant impact on heat distribution and thermal management processes. The velocity profile showcased uniform velocity at the inlet and increased velocity at the outlet, demonstrating the influence of porous wick on fluid flow dynamics. Overall, velocity proved to be a fundamental parameter influencing various aspects of fluid flow and heat transfer phenomena within the porous wick material.

Compliance with ethical standards

Disclosure of conflict of interest

No conflict of interest to be disclosed.

References

[1] Attinger, D., Frankiewicz, C., Betz, A. R., Schutzius, T. M., Ganguly, R., Das, A., ... & Megaridis, C. M. , 2014. Surface engineering for phase change heat transfer: A review. MRS Energy & Sustainability, 1(E4).

[2] Barnes, G., & Gentle, I. , 2011. Interfacial science: an introduction. USA: Oxford University Press.

[3] Chernysheva, M.; Maydanik, Y. , 2016. Effect of liquid filtration in a wick on thermal processes in a flat disk-shaped evaporator of a loop heat pipe. Int. J. Heat Mass Transf, Volume 106, p. 222–231.

[4] Deng, D.; Huang, Q.; Xie, Y.; Huang, X.; Chu, X. , 2017. Thermal performance of composite porous vapor chambers with uniform radial grooves. Appl. Therm. Eng. , Volume 125, p. 1334–1344.

[5] Faghri, A. , 2014. Heat pipes: review, opportunities and challenges. Frontiers in Heat Pipes (FHP), Volume 1, p. 5.

[6] Francisco, K.J.M.; Lago, C.L.D., 2018. Improving thermal control of capillary electrophoresis with mass spectrometry and capacitively coupled contactless conductivity detection by using 3D printed cartridges. Talanta, Volume 185, p. 37–41.

[7] Garimella, S. V., Persoons, T., Weibel, J. A., & Gektin, V., 2016. Electronics thermal management in information and communications technologies: Challenges and future directions. IEEE Transactions on Components, Packaging and Manufacturing Technology, Volume 7.

[8] Hasan, M. I. , 2020. Development of a Numerical Solver for Phase-Change and Two-Phase Flow in Porous Media. Master's thesis, University of Nevada, Reno.

[9] Kim, J.; Kim, S.J. , 2020. Experimental investigation on working fluid selection in a micro pulsating heat pipe. Energy Convers. Manag., Volume 205, p. 112462.

[10] Launay, S., Sartre, V., & Bonjour, J. , 2007. Parametric analysis of loop heat pipe operation: a literature review. International Journal of Thermal Sciences, 46(7), pp. 621-636.

[11] Launay, S.; Sartre, V.; Bonjour, J. , 2007. Parametric analysis of loop heat pipe operation: A literature review.. Int. J. Therm. Sci., Volume 46.

[12] Li, H.; Sun, Y. , 2018. Performance optimization and benefit analyses of a photovoltaic loop heat pipe/solar assisted heat pump water heating system. Renew. Energy , Volume 134, p. 1240–1247.

[13] Li, X.; Yao, D.; Zuo, K.; Xia, Y.; Yin, J.; Liang, H.; Zeng, Y.-P. , 2019. Fabrication, microstructural characterization and gas permeability behavior of porous silicon nitride ceramics with controllable pore structures.. J. Eur. Ceram. Soc. , Volume 39, p. 2855–2861.

[14] Li, Y., Lin, J., Xi, M., Wu, J., & Long, J. , 2023. Effects of surface nanotexturing on the wickability of microtextured metal surfaces. Journal of Colloid and Interface Science, Volume 638, pp. 788-800.

[15] Marchal, J. M., , 2001. Modeling Capillary Flow in Complex Geometries, Textile Research. Journal, Volume 71, pp. 813-821.

[16] Masoodi, R., & Pillai, K. M., 2013. Introduction to Wicking in Porous Media. Wicking in Porous Materials. Volume 1-12.

[17] Maydanik, Y. , 2005. Loop heat pipes. Appl. Therm. Eng. , Volume 25, p. 635–657.

[18] Maydanik, Y.; Chernysheva, M.; Pastukhov, V , 2014. Review: Loop heat pipes with flat evaporators. Appl. Therm. Eng. , Volume 67, p. 294–307.

[19] Mull, T., Wagner, T., Bonfigli, G., Buchholz, S., Schäfer, F., Schleicher, E., & Sporn, M. , 2022. Safety cases for design-basis accidents in LWRs featuring passive systems. Nuclear Engineering and Design, 111095(387).

[20] Seo, J., Kim, D., Kim, H., & Hassan, Y. A., 2022. An experimental investigation on the characteristics of heat pipes with annular type composite wick structure.. Nuclear Engineering and Design, Volume 390, p. 111701.

[21] Shi, X.; Yin, B.; Chen, G.; Zhang, X.; Mei, X, 2021. Numerical study on two-phase flow and heat transfer characteristics of loop rotating heat pipe for cooling motorized spindle. Appl. Therm. Eng. , Volume 192, p. 116927.

[22] Szymanski, P.; Law, R.; Glen RJ, M.; Reay, D.A. , 2021. Recent Advances in Loop Heat Pipes with Flat Evaporator. Entropy , Volume 23, p. 1374.

[23] Szymanski, P.; Mikielewicz, D. , 2022. Additive Manufacturing as a Solution to Challenges Associated with Heat Pipe Production. Materials , Volume 15, p. 1609.

[24] Tang, H.; Weng, C.; Tang, Y.; Li, H.; Xu, T.; Fu, T. , 2020. Thermal performance enhancement of an ultra-thin flattened heat pipe with multiple wick structure. Appl. Therm. Eng., Volume 183, p. 116203.

[25] Uwaoma, I. A. , 2021. Determination of Mass Flow Rate through Plain Mesh Wick and Nano-Structured Mesh Wick for the Design of Thermal Compressor Systems [Master's Dissertation], Oregon State University.

[26] Wadia, C., Alivisatos, A. P., & Kammen, D. M, 2009. Materials availability expands the opportunity for large-scale photovoltaics deployment. Environmental science & technology, 43(6), pp. 2072-2077.

[27] Wemp, C. K., & Carey, V. P. , 2017. Water wicking and droplet spreading on randomly structured thin nanoporous layers. Langmuir, 33(50), pp. 14513-14525.

[28] Wu, S.-Y.; Zheng, X.-F.; Xiao, L. , 2018. Phase change heat transfer characteristics of porous wick evaporator with bayonet tube and alkali metal as working fluid. Int. J. Therm. Sci. , , ., Volume 126, p. 152–161.

[29] Xu, G.; Xie, R.; Li, N.; Liu, C. J., 2021. Experimental Investigation of a Loop Heat Pipe With R245fa and R1234ze(E) as Working Fluids. Journal Therm. Sci. Eng. Appl. , Volume 14, p. 041014.

[30] Xu, J.; Wang, Z.; Xu, H.; Zhang, L. , 2017. Experimental research on the heat performance of a flat copper-water loop heat pipe with different inventories. Exp. Therm. Fluid Sci. , Volume 84, p. 110–119.